Low energy electron microscopy imaging using Medipix2 detectors

Sikharulidze, I.; Gastel, R. van; Schramm, S.; Abrahams, J.P.; Poelsema, B.; Tromp, R.M.; Molen, S.J. van der

Nuclear Instruments and Methods in Physics Research A 633 (2011) S239–S242

Contents lists available at ScienceDirect

Nuclear Instruments and Methods in Physics Research A

journal homepage: www.elsevier.com/locate/nima

Low energy electron microscopy imaging using Medipix2 detector

I. Sikharulidze [a,*,1], R. van Gastel [b,1], S. Schramm [c], J.P. Abrahams [a], B. Poelsema [b], R.M. Tromp [c,d], S.J. van der Molen [c]

[a] Leiden Institute of Chemistry, Leiden University, P.O. Box 9502, 2300RA Leiden, The Netherlands
[b] MESA+ Institute for Nanotechnology, University of Twente, P.O. Box 217, 7500AE Enschede, The Netherlands
[c] Kamerlingh Onnes Laboratory, Leiden University, P.O. Box 9504, 2300RA Leiden, The Netherlands
[d] IBM Research Division, T. J. Watson Research Center, P.O. Box 218, Yorktown Heights, NY 10598, USA

ARTICLE INFO

Available online 4 July 2010

Keywords:
Low energy electron microscopy
Photo-electron emission microscopy
Pixel detector

ABSTRACT

Low Energy Electron Microscopy (LEEM) and Photo-Emission Electron Microscopy (PEEM) predominantly use a combination of microchannel plate (MCP), phosphor screen and optical camera to record images formed by 10–20 keV electrons. We have tested the performance of a LEEM/PEEM instrument with a Medipix2 hybrid pixel detector using an Ir(1 1 1) sample with graphene flakes grown on its surface. We find that Medipix2 offers a number of advantages over the MCP. The adjustable threshold settings allow Medipix2 to operate as a noiseless detector, offering an improved signal-to-noise ratio for the same amount of signal compared to the MCP. At the same magnification Medipix2 images exhibit superior resolution and can handle significantly higher electron current densities than an MCP, offering the prospect of substantially higher frame rates in LEEM imaging. These factors make Medipix2 an excellent candidate to become the detector of choice for LEEM/PEEM applications.

1. Introduction

Low Energy Electron Microscopy (LEEM) [1,2] and Photo-Emission Electron Microscopy (PEEM) use backscattered or photo-emitted electrons, respectively, to analyse static and dynamic properties of sample surfaces. Traditionally, detectors comprising a micro-channel plate (MCP), phosphor screen and CCD camera are installed in LEEM/PEEM instruments [3]. Drawbacks of this detection scheme are the reduced resolution due to the use of phosphor screen, susceptibility of the MCP to damage in case of overexposure, and the intrinsic noise of CCD cameras. The alternative option of using a low noise CCD detector cannot provide video rate readout for measurements of dynamic effects.

Medipix2 is a hybrid pixel detector developed by the Medipix consortium [4], which has been successfully used in electron microscopy in the energy range up to 120 keV [5–7]. It features a high-resistivity silicon sensor bump-bonded to a CMOS ASIC chip. Each pixel has a separate analog pre-amplifier and a digital counter [8]. Low and high threshold values define the required amount of charge for triggering a count in the pixel [9]. This mechanism significantly reduces readout and background noise, resulting in a much improved dynamic range of the detector. Electrons in the 10–20 keV energy range provide enough charge for direct detection with Medipix2. The sensor layer above the ASIC chip also acts as a radiation shield and improves radiation hardness of the detector. Medipix2 can measure countrates above 100 kHz/pixel and can easily provide data for the video-rate readout.

2. Experimental

The measurements were performed on a Elmitec LEEM III instrument without energy filter, installed at the University of Twente. We used as a test sample Ir(1 1 1) with graphene flakes grown on its surface [10,11]. The coverage of the surface with graphene was around 40%. In the LEEM experiment the incident electrons were decelerated to 0–100 eV energy range by the strong field near the sample surface. The electrons that scattered from the surface, were accelerated up to 20 keV and guided via electro-optical system to the detector. In the PEEM measurements a Hg discharge lamp was used to induce electron emission from the graphene surface. The detection system on the original setup had a Chevron 3040FM MCP with bias voltage of 1350 V, a phosphor screen and a 12 bit PCO SensiCam CCD camera. The channel size of MCP was 10 μm and the spacing between channels was 12 μm. The resolution was 512 × 512 pixels with a circular detector area of 45 mm in diameter. The resolution limit for this system is around 3.5 linepairs/mm or 140 μm [12,13].

* Corresponding author.
E-mail address: irakli@chem.leidenuniv.nl (I. Sikharulidze).
[1] Both authors contributed equally to this work.

0168-9002/$ - see front matter © 2010 Elsevier B.V. All rights reserved.
doi:10.1016/j.nima.2010.06.177

The Medipix setup featured a single chip Medipix2 (MXR) [8] on a CERN carrier board with USB 1.1 readout electronics [14]. The image resolution was 256×256 pixels with square detector area of $14 \times 14\,mm^2$ and pixel size of $55\,\mu m$, which is approximately three times smaller than for MCP. Initially, reference images were recorded using the original MCP setup. Subsequently, the imaging column was opened and the MCP setup was replaced with a custom designed adapter flange containing the Medipix2 detector with the readout electronics board (see Fig. 1). Both the chipboard and the readout board were operating inside the imaging column under UHV conditions. Extensive degassing led to a substantial drop in the vacuum level to 4×10^{-7} mbar with the detector switched off and to 2×10^{-6} mbar during the measurements. The Medipix2 chip was around 20 mm further down the column compared to the MCP, leading to minor readjustments in the focusing system for optimal image collection. A flat-field mask, used for correction of the Medipix images, was measured by defocusing the original LEEM/PEEM image to achieve maximally homogeneous detector illumination. Data from the Medipix 2 were collected using the Pixelman software [15] and analysed with the SciPy software package [16].

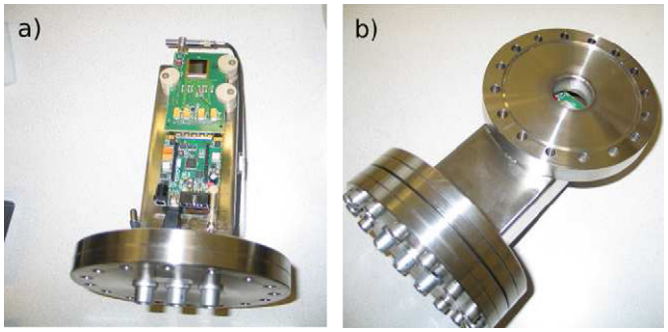

Fig. 1. (a) The Medipix2 chipboard with the readout electronics clamped to the metal holder. (b) The assembled unit ready for installation into LEEM instrument.

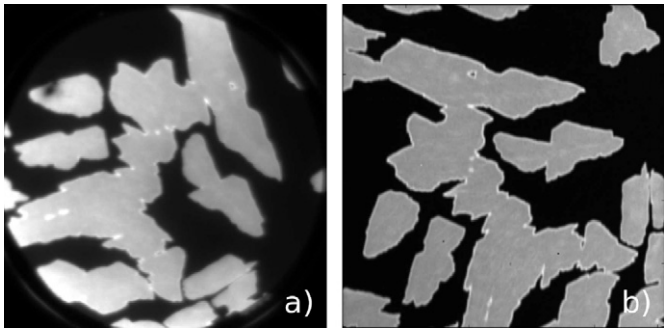

Fig. 2. PEEM images of the graphene flakes on the surface of Ir(1 1 1). The images were recorded using (a) the MCP setup with 50 μm FoV and (b) the Medipix2 with 150 μm FoV settings.

3. Results and discussion

Fig. 2 depicts the sample area recorded using the MCP and Medipix based PEEM setups. In order to compensate for the smaller area of the Medipix2 detector, the data were recorded at the three times larger field-of-view (FoV) value compared to the corresponding MCP image. Nevertheless, the Medipix2 image provided superior resolution and contrast compared to the MCP data.

A photon energy of 4.8 eV was used to generate photo-electron emission. This value was higher than the graphene work function (4.5 eV) but lower than the Ir(1 1 1) work function (5.3 eV). Consequently, the graphene areas in Fig. 2 appear bright and the Ir(1 1 1) surface appears dark. Difference of the work function between graphene and Ir(1 1 1) creates field gradient at the edges of graphene islands. This results in brightening of the graphene flake contours in PEEM images, particularly evident on the Medipix image in Fig. 2b.

LEEM images recorded with the MCP setup for several FoV settings are presented in Fig. 3. The corresponding Medipix images are shown in Fig. 4. Examining the images with the same FoV settings one notices that the structural features on the surface are more clearly visible with the Medipix2 detector. Quantitative comparison of the step widths on the surface of Ir(1 1 1) indicates about a factor 2 improvement in resolution of Medipix over MCP [11]. In Fig. 4a, edges of the graphene layers with their characteristic angles of 120° are well resolved. These features are not visible in the corresponding Fig. 3a, also not if we zoom in, and become apparent only in Fig. 3b. In the corresponding Medipix image, Fig. 4b, one can already resolve defects on the Ir(1 1 1) surface that are not visible in Fig. 3b. Lack of distinctive features in the MCP image at the higher magnification and small size of the Medipix2 chip made it impossible to get the images of the same surface area with both detectors at smaller FoV. Nevertheless, one can see that a screw dislocation on Ir(1 1 1) surface, captured in the middle of Fig. 4c, is well resolved, while the similar features in Fig. 3c are less evident.

Operation of the Medipix 2 detector was assessed by performing a calibration of low threshold DAC values (THL) and by looking at the dependence of the countrate on the bias voltage applied to the sensor. Threshold dependencies were collected in the PEEM measurements. The derivatives of the threshold scans plotted in Fig. 5 are related to the spectral properties of the incident radiation [17]. Positions of the maxima in the derivative

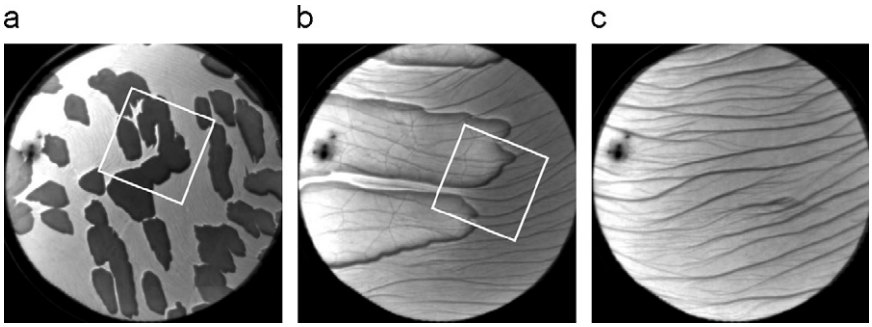

Fig. 3. LEEM images obtained with the MCP setup at the (a) 50 μm, 7.1 eV, (b) 10 μm, 7.1 eV and (c) 6 μm, 5.0 eV FoV and energy settings.

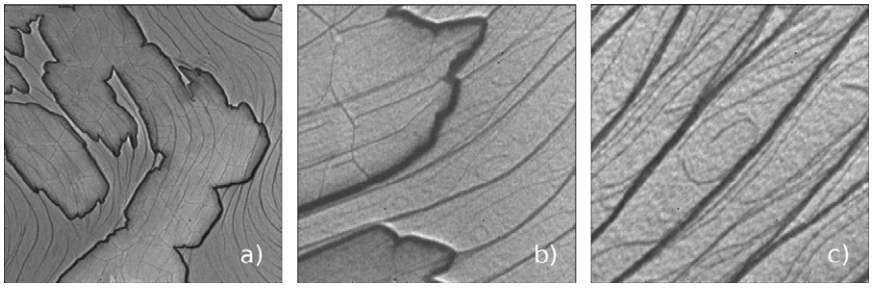

Fig. 4. Medipix2 images of the areas indicated by the white squares in Fig. 3, obtained with the same FoV and energy settings of the LEEM instrument.

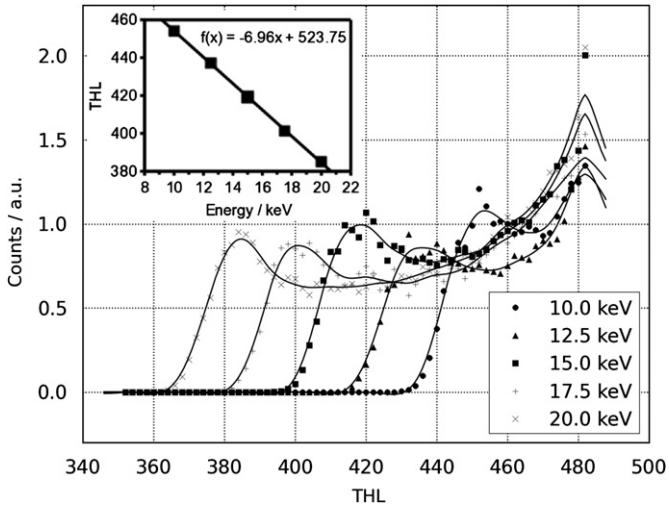

Fig. 5. Derivatives of the THL scans measured for the different acceleration voltages in the PEEM experiment. The resulting curves were smoothed using splines. Position of the peak in each curve corresponds to the setting of acceleration voltage. Inset: THL calibration obtained from the positions of maxima in the derivatives of the THL scans.

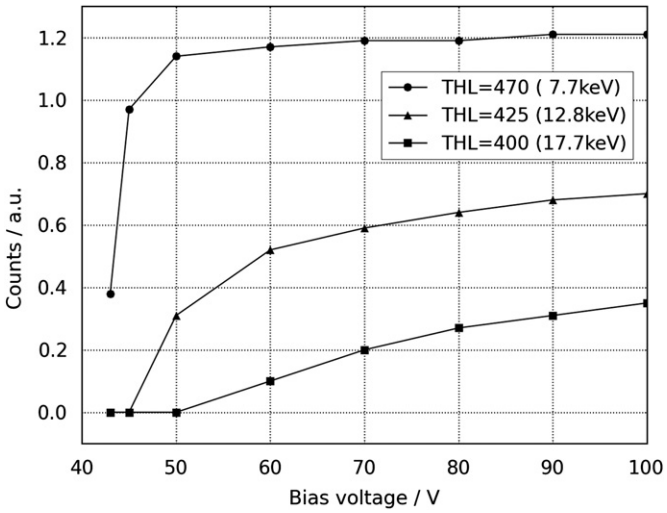

Fig. 6. Medipix2 countrate dependence on bias voltage for the three threshold settings.

curves, which correspond to the energy of electrons set by the acceleration voltage in the PEEM experiment, can be used to calibrate THL values in terms of energy. The resulting calibration curve shown in the inset in Fig. 5 indicates linear dependency of the THL setting on the electron energy, which is consistent with the expected behaviour of Medipix 2. We recorded the countrate dependence on the bias voltage for several threshold settings. The results are shown in Fig. 6. With decreasing bias voltage, the charge generated inside the sensor layer diffuses over a wider area, reducing the charge collected per pixel. Subsequently, the countrate decreases with decreasing bias voltage. This effect becomes more evident for higher threshold settings. Reduction of the sensor thickness would limit the available volume for charge diffusion, but we did not test this hypothesis. Electrons of 20 keV have a range of only few microns inside silicon. Having an excessively thick (300 μm) sensor layer, which was designed with X-ray applications in mind, only reduces resolution and could also result in lower countrate. Thinning the sensor layer could further improve the performance of Medipix in LEEM/PEEM experiments [18].

4. Conclusions

Medipix2 was successfully used for LEEM/PEEM imaging. Improved resolution and contrast allowed us to record features on the graphene and Ir(1 1 1) surfaces that could not be resolved at the same instrument settings using an MCP based system. The threshold mechanism implemented in Medipix2 substantially increases the dynamic range of the detector and it can provide image data at video-rate speed. These features make Medipix our detector of choice in LEEM/PEEM instruments. The limiting factors in the present experiment were incompatibility of the electronics design with the UHV conditions and readout electronics which did not utilize full speed of the Medipix2 chip. Both of these issues are addressed by the new Medipix carrier [19] and readout board [20] prototypes developed within Medipix consortium. Tiling of Medipix chips is also actively pursued, with the first 'Quad'-detectors provided by RELAXd project [21]. Medipix detector performance in LEEM/PEEM could be further improved by using thinner silicon sensor layer.

Acknowledgments

This research was funded by the Netherlands Organization for Scientific Research (NWO) via an NWO-Groot grant ('ESCHER') as well as by the Dutch Foundation for technical sciences (STW) and the Cyttron consortium. We gratefully acknowledge Ruud van Egmond, Emiel Wiegers and Ewie de Kuyper for technical support. We thank Jan van Ruitenbeek, Wasi Faruqi, Jan Visser, Jan Visschers and Erik Heijne for inspiring discussions. We would like to acknowledge members of Medipix consortium for their advice and support.

References

[1] E. Bauer, Surf. Sci. 299–300 (1994) 102.
[2] R.M. Tromp, IBM J. Res. Dev. 44 (4) (2000) 503.
[3] W. Telieps, E. Bauer, Ultramicroscopy 17 (1) (1985) 57.
[4] ⟨http://www.cern.ch/medipix/⟩.
[5] G. McMullan, D. Cattermole, S. Chen, R. Henderson, X. Llopart, C. Summerfield, L. Tlustos, A. Faruqi, Ultramicroscopy 107 (4–5) (2007) 401.
[6] G. McMullan, S. Chen, R. Henderson, A. Faruqi, Ultramicroscopy 109 (9) (2009) 1126.
[7] A. Faruqi, R. Henderson, L. Tlustos, Nucl. Instr. and Meth. A 546 (1–2) (2005) 160.
[8] X. Llopart, M. Campbell, R. Dinapoli, D.S. Segundo, E. Pernigotti, IEEE Trans. Nucl. Sci. NS-49 (5) (2002) 2279.
[9] L. Tlustos, R. Ballabriga, M. Campbell, E. Heijne, K. Kincade, X. Llopart, P. Stejskal, IEEE Trans. Nucl. Sci. NS-53 (1) (2006) 367.
[10] J. Coraux, A.T. N'Diaye, M. Engler, C. Busse, D. Wall, N. Buckanie, F.-J.M. zu Heringdorf, R. van Gastel, B. Poelsema, T. Michely, New J. Phys. 11 (2) (2009) 023006.
[11] R. van Gastel, I. Sikharulidze, S. Schramm, J.P. Abrahams, B. Poelsema, R. Tromp, S.J. van der Molen, Ultramicroscopy 110 (1) (2009) 33.
[12] H. Shimizu, T. Yasue, T. Koshikawa, in: Proceedings of the 6th International Symposium on Atomic Level Characterizations for New Materials and Devices ALC'07, Kanazawa, Japan, p. 203.
[13] G. Moldovan, J. Matheson, G. Derbyshire, A. Kirkland, Nucl. Instr. and Meth. A 596 (3) (2008) 402.
[14] Z. Vykydal, J. Jakubek, S. Pospisil, Nucl. Instr. and Meth. A 563 (1) (2006) 112.
[15] T. Holy, J. Jakubek, S. Pospisil, J. Uher, D. Vavrik, Z. Vykydal, Nucl. Instr. and Meth. A 563 (1) (2006) 254.
[16] E. Jones, T. Oliphant, P. Peterson, et al., SciPy: Open source scientific tools for Python (2001-). ⟨http://www.scipy.org/⟩.
[17] L. Tlustos, Performance and limitations of high granularity single photon processing X-ray imaging detectors, Ph.D. Thesis, University of Technology, Vienna, 2005.
[18] E. Heijne, private communication.
[19] J. Visser, J. Visschers, private communication.
[20] M. Platkevic, V. Bocarov, J. Jakubek, S. Pospisil, V. Tichy, Z. Vykydal, Nucl. Instr. and Meth. A 591 (1) (2008) 245.
[21] Z. Vykydal, J. Visschers, D.S. Tezcan, K.D. Munck, T. Borgers, W. Ruythooren, P.D. Moor, Nucl. Instr. and Meth. A 591 (1) (2008) 241.